# A statistical health monitoring and forecasting framework for transportation infrastructure

Yikai Chen and Pablo Durango-Cohen

Department of Civil and Environmental Engineering

Northwestern University

2145 Sheridan Road, Room A332, Evanston, IL 60208-3109

(847) 491-4008

pdc@northwestern.edu

## ABSTRACT

In this paper, we propose a framework to monitor distress conditions of multiple structural facilities simultaneously. Multivariate statistical process control methods were employed to: 1) reduce the dimension of data; 2) capture the interrelations among distresses and; 3) rigorously control the false alarm rate. We implemented the methods to monitor the long-term fatigue process of the Hurley Bridge on the border of Wisconsin and Michigan. Real-time measurements were collected on the strains and displacements at critical locations of the bridge over two years. Weather and traffic conditions were sampled over the same period to account for exogenous factors. Empirical studies signaled suspicious events with 99% confidence and interpreted their plausible sources. The results indicate that the proposed framework is effective in field practices.

## 1. INTRODUCTION

Health monitoring of field infrastructures has interested researchers for several decades. Recent advancement in wireless technologies has made long-term real-time monitoring applicable at reasonable costs, and prompted the need for state-of-the-art methods to analyze and interpret the data. The primary goal is to ensure the longevity and safety of infrastructure and to optimize resource allocation.

Chen et al. *(1)* proposed a statistical framework to monitor the deterioration conditions of individual facilities, i.e. distresses. The framework treats the variation in the deterioration conditions as a combination of common-cause variation and special-cause variation. The former refers to changes that can be explained and predicted by usual, and often recurrent, operational conditions; the latter refers to changes attributed to extraordinary events. We took a two-step approach to analyze these two variation components respectively. In the first step, we formulated performance models to describe and predict common-cause variation in a distress and decompose it into linear trends, seasonality, systematic patterns, and residuals. In the second step, we used Shewhart control charts to detect special changes in the residuals series.

The main contribution of the paper herein is to bring the second step in *(1)* forward to monitor multiple distresses together as a group. The main motivations to use multivariate methods include the following: First, to reduce the dimension of data. For example, if we are monitoring 10 distresses, then we have 10 separate sets of control charts to be computed, visualized, and managed. This is not efficient. In contrast, using multivariate method will integrate them into a central set of chart that is more manageable. Second, the behaviors of multiple distresses are usually interrelated, which represents the structural nature of the underlying facility. So it is desirable to capture those redundancies for comprehensive monitoring and effective decision-making. Unfortunately, the separate univariate charts will likely lose that information. Third, when we alarm the out-of-control signals, we want to control the type-I error rate to ensure rigorous inferences. The type-I error rate is a confidence level that defines the probability of false alarms, and we want to keep it small. However, if we use separate univariate charts to monitor multiple variables, the overall type-I error rate will be either larger than the predetermined confidence level or very difficult to calculate.

Motivated by these factors, we introduce the idea of Multivariate Statistical Process Control (MSPC). It refers to a set of advanced techniques for the monitoring and control of the operating performance of batch and continuous processes. More specifically, it reduces the information contained within all of the process variables down to two or three composite metrics through the application of statistical modeling. These composite metrics can then be easily monitored in real time in order to benchmark process performance and highlight potential problems, thereupon providing a framework for continuous improvement of the process operation. Harold Hotelling established multivariate process control techniques in his 1947 pioneering paper *(2)*. He proposed the Hotelling's $T^2$ control chart, which takes into account that a change in one variable can cause a rippling effect throughout the system. The control charts is based on a scalar statistic that measures how far a multivariate process is away from its target values. Since its development, the chart has been used to evaluate, monitor and control processes in a wide range of areas such as manufacturing, finance, healthcare, customer service, etc.

The remainder of the paper is organized as follows. Section 2 proposes the methodological framework. Section 3 provides an empirical study to validate the framework. We conclude our paper in Section 4.

## 2. METHOD

In this section, we describe the methods used to develop multivariate control charts. We start with deriving the Hotelling's $T^2$ statistic and then use it to construct a corresponding control chart that monitors multiple distress behaviors. We further introduce a primary method to identify the source variable(s) for out-of-control signals in the $T^2$ control chart.

### 2.1 Constructing the Multivariate Control Chart

In a univariate control chart, the core concept is to measure how far a sample point is away from the target value or the mean level obtained from a group of historic data. Similarly, the core concept of a multivariate control chart is to measure how far a sample vector is away from a target vector, or a mean vector obtained from the historic data set. In addition to the increased dimension, a big difference between the two measurement scenarios is that the latter one needs to take into account the associated covariance among the variables. Also, although we are measuring the distance between multivariate vectors, it is desirable to convert the result into a scalar value so that we can conveniently make comparisons and visualization. Mahalanobis *(3)* proposed such a measurement method when the true parameters (mean and covariance structure) of the historic data set are known. Following the same idea, Harold Hotelling *(2)* proposed the $T^2$ statistic to serve the same purpose when the parameters are unknown.

#### 2.1.1 Mahalanobis Distance

For a multidimensional vector $X$, the Mahalanobis distance $D_M$ measures its divergence from the mean vector $\mu$ of a given group of sample vectors, taking into account the covariance structure associated. The distance can be formulated as:

$$D_M = \sqrt{(X-\mu)' \cdot \Sigma^{-1} \cdot (X-\mu)} \tag{1}$$

where $\Sigma$ is the covariance matrix among the sample vectors.

Now let us apply the Mahalanobis distance to monitoring quality characteristics. Assume we are monitoring the characteristic of $p$ variables over $m$ sampling periods, and for each variable we observe $n > 1$ measurements in each sampling period. We regard the $n$ observations as a subgroup of data, and denote the subgroup mean value of variable $k$ at sampling period $j$ as:

$$\bar{x}_{jk} = \frac{1}{n} \cdot \sum_{i=1}^{n} x_{ijk}, \qquad \begin{matrix} j = 1,2,\cdots,m \\ k = 1,2,\cdots,p \end{matrix} \tag{2}$$

where $x_{ijk}$ is the $i$th measurement point in the subgroup ($i = 1,2,\cdots,n$). If we arrange the subgroup mean values for all the $p$ variables together, it will form a $p$- dimensional vector:

$$\bar{X}_j = \left[\bar{x}_{j1}, \bar{x}_{j2}, \cdots \bar{x}_{jp}\right]' \tag{3}$$

that integrates all the quality characteristics information at sampling period $j$. Since $\bar{X}_j$ is a random variable, we can define a statistic to measure its distance from a known mean vector $\mu$ and a known covariance matrix $\Sigma$ along the $p$ characteristics:

$$\chi_j^2 = n \cdot \left(\bar{X}_j - \mu\right)' \cdot \Sigma^{-1} \cdot \left(\bar{X}_j - \mu\right), \qquad j = 1,2,\cdots,m \tag{4}$$

$\chi_j^2$ is a one-dimensional random variable, and it is the squared value of the Mahalanobis distance between $\bar{X}_j$ and $\mu$ multiplying the subgroup size $n$. In addition, it can also be shown *(4)* that $\chi_j^2$ follows a

chi-square distribution with $p$ degrees of freedom if the characteristics of $\bar{X}_j$ is consistent with the given parameters.

### 2.1.2 Hotelling's $T^2$ Statistic

The $\chi^2$ statistic presented above can only apply to situations when parameters $\mu$ and $\Sigma$ of the quality monitoring process are known. However, in many practical applications, this is not the case. Therefore we need to estimate the parameters using the sample data. Harold Hotelling *(2)* proposed the Hotelling's $T^2$ statistic to serve this purpose. Similar to the $\chi^2$ statistic, the $T^2$ statistic regards multiple quality characteristics as a simultaneous group of variables that interact with each other and synthesize them into a scalar variable.

We consider the situation where subgroup size $n > 1$. Following the same notation as above, the $T^2$ statistic at sampling period $j$ can be formulated as:

$$T_j^2 = n \cdot \left(\bar{X}_j - \hat{\mu}\right)' \cdot S^{-1} \cdot \left(\bar{X}_j - \hat{\mu}\right) \tag{5}$$

where $\hat{\mu}$ is the sample mean vector, $S$ is the sample covariance matrix and $\bar{X}_j$ is defined in equation (3). We describe the calculation of $\hat{\mu}$ and $S$ below.

An overall estimate of the mean of variable $k$ is obtained by averaging across all the $m$ subgroup means:

$$\bar{\bar{X}}_k = \frac{1}{m} \cdot \sum_{j=1}^{m} \bar{x}_{jk}\,, \qquad k = 1,2,\cdots,p \tag{6}$$

Repeating this for all the $p$ variables we obtain an unbiased estimate of the mean vector:

$$\hat{\mu} = \left[\bar{\bar{X}}_1, \bar{\bar{X}}_2, \cdots, \bar{\bar{X}}_p\right]' \tag{7}$$

To estimate the covariance matrix $\Sigma$, we start with calculating the subgroup variances and covariance. For the $j$th group of variable $k$, the sample variance $s_{jk}^2$ within the group is calculated as:

$$s_{jk}^2 = \frac{1}{n-1} \cdot \sum_{i=1}^{n} \left(x_{ijk} - \bar{x}_{jk}\right)^2 \tag{8}$$

Similarly, an estimate of the covariance between variable $k$ and variable $l$ at sampling period $j$ is calculated as:

$$s_{jkl} = \frac{1}{n-1} \cdot \sum_{i=1}^{n} \left(x_{ijk} - \bar{x}_{jk}\right) \cdot \left(x_{ijl} - \bar{x}_{jl}\right), \qquad k \neq l \tag{9}$$

An overall estimate of the variance of variable $k$ and the covariance between variable $k$ and variable $l$ can be obtained by averaging the subgroup variances and covariance across all the $m$ subgroups:

$$\bar{s}_k^2 = \frac{1}{m} \cdot \sum_{j=1}^{m} s_{jk}^2\,, \qquad k = 1,2,\cdots,p \tag{10}$$

$$\bar{s}_{kl} = \frac{1}{m} \cdot \sum_{j=1}^{m} s_{jkl}\,, \qquad k \neq l \tag{11}$$

Repeating this for all the $p$ variables we obtain an unbiased estimate of the covariance matrix $\Sigma$. Denoting this estimate matrix as $S$, we have:

$$S = \begin{bmatrix} \bar{s}_1^2 & \bar{s}_{12} & \cdots & \bar{s}_{1p} \\ & \bar{s}_2^2 & \cdots & \bar{s}_{2p} \\ & & \ddots & \vdots \\ & & & \bar{s}_p^2 \end{bmatrix} \tag{12}$$

Therefore, the $T^2$ statistic at sampling period $j$ is calculated by equation (5) with the estimated $\hat{\mu}$ and $S$. If the monitored quality characteristics derive from random processes and follow a $p$-variate normal distribution, it can be shown that the $T^2$ statistic follows an $F$ distribution with a constant multiple:

$$T_j^2 \sim \frac{(m\pm1)\cdot(n-1)\cdot p}{m\cdot(n-1)-p+1} \cdot F_{p,m(n-1)-p+1}, \qquad j = 1,2,\cdots,m \tag{13}$$

Note that the $\pm$ sign takes positive when $\bar{X}_j$ represents a newly observed sample that is not included to calculate the overall sample mean vector $\hat{\mu}$, and negative otherwise *(4)*.

## 2.2 Charting the $T^2$ Statistic

Control charting introduced by Shewhart *(6)* is a widely used tool to monitor quality processes. The basic procedure includes data organization, choosing the appropriate charting statistic, determining the desired type-I error rate, computing the control limits, and alarming the out-of-control signals. As is in the univariate application, there are two distinct phases in monitoring a multivariate quality process *(7)*. Phase *I* takes a retrospective review at the historic data samples, determining whether they come from an in-control process. An important goal of this phase is to obtain a set of reference samples so that reliable control limits can be computed accordingly. In this sense, Phase *I* is also regarded as a start-up stage of the monitoring procedure. Phase *II* presents a prospective review for future data to monitor whether the process remains in control.

As is described in the previous section, the $\chi^2$ statistic provides an effective measure of the divergence of a multivariate sample from the mean level, and the $T^2$ statistic is a practical alternative when the true parameters are unknown. We use it to construct the multivariate control chart.

Once we have collected and organized data for phase *I*, we can calculate the $T^2$ value for each sampling period to be monitored. Since we are monitoring a series of squared values, we only need an upper control limit which is defined as:

$$\mathrm{UCL}_I = \frac{(m-1)\cdot(n-1)\cdot p}{m\cdot(n-1)-p+1} \cdot F_{\alpha,p,m(n-1)-p+1} \tag{14}$$

where $\alpha$ is the desired type-I error rate and $F_{\alpha,p,m(n-1)-p+1}$ is the $(1-\alpha)$ quantile of the $F$ distribution with degrees of freedom $p$ and $m(n-1)-p+1$, *(7)*. In fact, this equals to testing a hypothesis in response to the distribution statement in equation (13)

$$H_0: T_j^2 \sim \frac{(m-1)\cdot(n-1)\cdot p}{m\cdot(n-1)-p+1} \cdot F_{p,m(n-1)-p+1}$$

against its alternative at the $\alpha$ confidence level. Note that the $\pm$ sign takes negative here because each of the samples in phase *I* is used in estimating the mean vector $\hat{\mu}$. The choice of $\alpha$ should be determined based on the acceptable false alarm rate over the designed monitoring procedure. In many cases the values is fixed at $\alpha = 0.27\%$ following the traditional $3\sigma$ standard used in Shewhart control charts. In other word, it allows 3 false alarms in every 1000 samples.

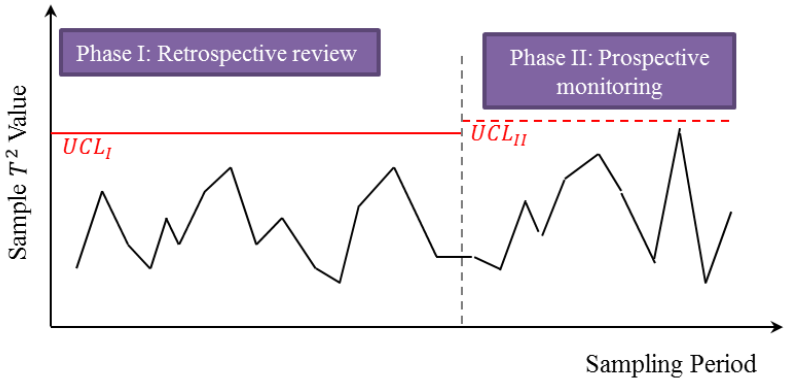


FIGURE 1 $T^2$ Control Chart of Both Phases

We lay out the $T^2$ values over a horizontal line and superimpose the $\text{UCL}_I$ computed above (Figure 1). Any point beyond the control limit triggers an out-of-control signal. We record the signals for further explanation, remove them from the phase *I* control chart, and recalculate the $\text{UCL}_I$ using the remaining data. We repeat this process until no signals are detected.

When quality characteristics data for phase *II* are available, we calculate their $T^2$ values and lay them over the extended horizontal line (Figure 1). The upper control limit for phase *II* is defined as:

$$\text{UCL}_{II} = \frac{(m+1)\cdot(n-1)\cdot p}{m\cdot(n-1)-p+1} \cdot F_{\alpha,p,m(n-1)-p+1} \tag{16}$$

Note that the $\text{UCL}_{II}$ here is different than the $\text{UCL}_I$ in equation (15) since it adopts $(m+1)$ rather than $(m-1)$ in the numerator. This reflects the fact that the monitored samples in phase *II* are not used to estimate the mean vector $\hat{\mu}$. Any point beyond $\text{UCL}_{II}$ triggers an out-of-control signal in this phase.

### 2.3 A Special Case: Bivariate Distress Monitoring

Consider a bivariate observation $Z = [x, y]'$. Denote the unknown mean vector of the observation by $\mu = [\mu_x, \mu_y]'$ and the unknown covariance relationship by:

$$\Sigma = \begin{bmatrix} \sigma_x^2 & \sigma_{xy} \\ \sigma_{yx} & \sigma_y^2 \end{bmatrix} \tag{17}$$

where $\sigma_{xy} = \sigma_{yx}$ represents the covariance between the two variables. The correlation between the two variables is given by $\rho = \sigma_{xy}/\sigma_x\sigma_y$.

Hotelling's statistic converts the observation vector $Z$ into a univariate control statistic $T^2$. Its mathematical form is given as:

$$\begin{aligned} T^2 &= n \cdot (Z-\mu)' \cdot \Sigma^{-1} \cdot (Z-\mu) \\ &= \frac{n}{1-\rho^2} \cdot \left[ \frac{(x-\mu_x)^2}{\sigma_x^2} - 2\rho \cdot \frac{(x-\mu_x)}{\sigma_x} \cdot \frac{(y-\mu_y)}{\sigma_y} + \frac{(y-\mu_y)^2}{\sigma_y^2} \right] \end{aligned} \tag{18}$$

When the equation is set equal to a constant, it depicts an ellipse as is illustrated graphically in Figure 2. The horizontal and vertical axis of the plane in Figure 2 corresponds to variable $x$ and variable $y$

respectively. The dashed lines represent the two pairs of univariate control limits, and the solid ellipse represents the bivariate $T^2$ control limit defined in equation (18). Interestingly, the ellipse is tilted when variables $x$ and $y$ are interrelated and flat if they are independent to each other.

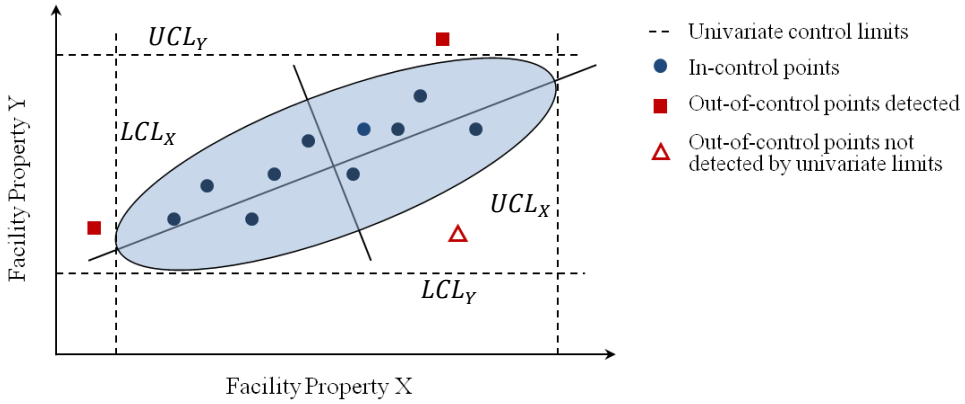


FIGIRE 2 Elliptical Control Region for Bivariate Chart

## 2.4 Interpreting Out-of-control Signals

Not similar to univariate control charts where each out-of-control signal is exclusively linked to a unique variable, in multivariate control charts, the interpretation (i.e., the root cause) of signals is not clear by looking at the chart itself. For example, an observation may be detected as out-of-control in the $T^2$ chart because one or more of the individual variables is outside their respective control boundaries. Alternatively, such a multivariate signal could also occur when two or more individual variables do not adhere to the established correlation structure. An even more complicated situation is when the signal stems from a combination of the two situations above, with some variables being outside their boundaries and others being counter-correlated.

As a result, it is of primary interest to identify the main sources of the signals in the $T^2$ control chart. In other words, we need to know which variable(s) have significantly contributed to the large value in the $T^2$ statistic.

Researchers have proposed several solutions to address this problem. Interested readers are referred to *(8)*, *(9)* and *(10)*. In this paper we implement the Mason-Young-Tracy (MYT) Decomposition to analyze and interpret the multivariate signals in the $T^2$ control chart.

### 2.4.1 Decomposition

One method to interpret the signals in $T^2$ control chart was given by Mason et al. in *(11)* and *(12)*. The idea is to decompose the signaled $T^2$ value into orthogonal terms that represent contributions from different individual variables. Any term that exceeds a determined threshold indicates that the associated variables have contributed significantly to the signal.

**Bivariate decomposition**

As a simpler example, let's look at a bivariate case where $x_1$ and $x_2$ are two interdependent quality characteristics. At any sampling period, the MYT method decomposes the total $T^2$ value into two orthogonal and equally weighted terms:

$$T^2 = T_1^2 + T_{2|1}^2 \tag{19}$$

where $T_1^2$ represents the marginal contribution of $x_1$ to the total $T^2$ value as if $x_2$ is disregarded, and $T_{2|1}^2$ represents the additional contribution of $x_2$ when the value of $x_1$ is fixed. The calculation of the two components is given by:

$$T_1^2 = n \cdot \frac{(x_1 - \bar{x}_1)^2}{s_1^2} \tag{20}$$

$$T_{2|1}^2 = n \cdot \frac{(x_2 - \bar{x}_{2|1})^2}{s_{2|1}^2} \tag{21}$$

where $\bar{x}_{2|1}$ is an estimate of the mean level of $x_2$ conditioned on a given value of $x_1$, $s_{2|1}^2$ is the corresponding estimate of the variance of $x_2$ conditioned on the given $x_1$, and $n > 1$ is the number of observations in each sample.

Symmetrically, we can also decompose the total $T^2$ value as:

$$T^2 = T_2^2 + T_{1|2}^2 \tag{22}$$

with the formulation and statistical explanation switched around between $x_1$ and $x_2$. Equation (19) and (22) look at the same problem from opposite perspectives and they serve as two alternative anatomies of $T^2$. Based on their statistical nature, we denote the first term in both equations (i.e., $T_1^2$ and $T_2^2$) as the marginal or unconditional component of $T^2$ and the second terms (i.e., $T_{2|1}^2$ and $T_{1|2}^2$) as the condition components.

The statistical interpretation is: a large value in marginal components indicates an outlier in the corresponding variable, while a large value in the conditional components indicates a break of the relationship among the involved individual variables. In order to determine a threshold for consistent judgment, Mason et al. *(11)* showed that both marginal and conditional components follow an *F* distribution times a constant:

$$T_*^2 \sim \frac{m+1}{m} \cdot F_{1,m(n-1)} \tag{23}$$

if nothing unusual happens to the related components. Here "$*$" represents all the four $T^2$ components in the bivariate case, $m$ is the number of sample periods and $n$ is the number of observations in each sample. Therefore, we can compare the $T^2$ components calculated by equation (20) and (21) with the determined thresholds above to evaluate the contributions of each component. A more detailed explanation of the bivariate MYT method can be found in *(12).*

**P-variate decomposition**

For p-variate situations, the decomposition in equation (19) can be generalized to:

$$T^2 = T_1^2 + T_{2|1}^2 + T_{3|1,2}^2 + \cdots + T_{p|1,2,\cdots,p-1}^2 \tag{24}$$

where $T_k^2$ is the $T^2$ statistic calculated using only the first $k$ variables, and the conditional term $T_{k+1|1,2,\cdots,k}^2$ represents the additional contribution of variable $k+1$ when variable 1 through $k$ are fixed ($k = 1,2,\cdots,p-1$). The formulation and detailed explanation can be found in *(11)*.

Equation (24) is one of the many ways to partition the overall $T^2$ statistic. A different partition could be:

$$T^2 = T_2^2 + T_{1|2}^2 + T_{3|1,2}^2 + \cdots + T_{p|1,2,\cdots,p-1}^2 \tag{25}$$

Since each partition involves $p$ terms, Mason et al. showed that there are in total $p!$ different ways to partition $T^2$. In addition, it is worth noting that the order of conditional terms does not matter, that is:

$$T_{k+1|1,2,\cdots,k}^2 = T_{k+1|2,1,\cdots,k}^2 \tag{26}$$

Taking that into account, there are $p \cdot 2^{(p-1)}$ unique component terms involved over the entire decomposition scheme. Similar to the bivariate case, all of the components follow a predetermined distribution with a multiple if no unusual change happens within the associated variables.

## 3. EMPIRICAL STUDY

In this section, we apply the multivariate control charting method described above to monitor the distress measurements on the Hurley Bridge. The bridge carries westbound USH-2 traffic over the Montreal River from Ironwood, Michigan into Hurley, Wisconsin. It is a three-span continuous five-girder steel structure with a composite deck. Figure 3 illustrates a structural layout of the Hurley Bridge as well as a profile of the sensor deployment on it. A detailed list of the bridge components that are measured as well as their locations is given in Table 1.

For each distress, we collected data from April 1st, 2010 through December 20th, 2011, a total of 628 days, as a sample set for numerical analyses. The measurements were sampled at 100Hz, and they were averaged on an hourly basis by the on-site computer processor before we obtained the data. In addition to the distress measurements, we simultaneously collected the environmental conditions: steel temperatures, air temperature, and relative humidity in the same data set. A description of these exogenous variables is also listed in Table 1.

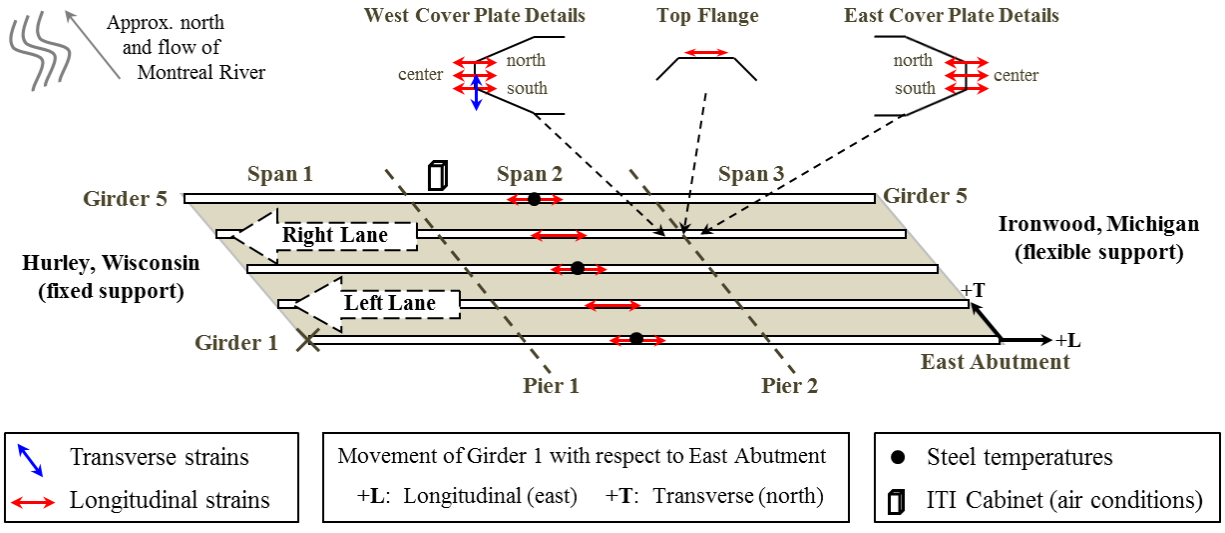


FIGURE 3 Structural Layout and Sensors Deployment of the Hurley Bridge

In the rest of this section, we illustrate the results of a bivariate study on the biaxial displacements at the east side of girder 1 (denoted Displ-L and Displ-T respectively) as an example.

**TABLE 1 Description of Instrumentation on the Hurley Bridge**

| Instrument | Measurement | Unit | Component | Location |
|---|---|---|---|---|
| Displ-L<br>Displ-T | Displacement | mils | Girder 1 | East abutment |
| G1-S2-M | Strain | $\mu$strain | Girder 1 | Span 2, mid-point |
| G2-S2-M | | | Girder 2 | |
| G3-S2-M | | | Girder 3 | |
| G4-S2-M | | | Girder 4 | |
| G5-S2-M | | | Girder 5 | |
| G4-P2-TF | | | Girder 4 top flange | Pier 2 |
| G4-WCP-SL<br>G4-WCP-ST | | | Girder 4 top flange cover plate | Pier2, west end south edge |
| G4-WCP-CL | | | | Pier 2, west end center |
| G4-WCP-NL | | | | Pier 2, west end north edge |
| G4-ECP-SL | | | | Pier 2, east end south edge |
| G4-ECP-CL | | | | Pier 2, east end center |
| G4-ECP-NL | | | | Pier 2, east end north edge |
| ST-G1 | Steel temperature | $^oF$ | Girder 1 | Span 2, mid-point |
| ST-G3 | | | Girder 3 | |
| ST-G5 | | | Girder 5 | |
| Temp | Air temperature | $^oF$ | | |
| Humid | Relative humidity | % | | |

### 3.1 Multivariate Control Charts

For each distress, we calculated the daily conditions by averaging the hourly measurements during the day, and then further organized the daily conditions into weekly subgroup samples. In other word, a subgroup sample includes 7 observation points, each of them representing the average daily condition of the underlying characteristic. Therefore we had 628/7 = 89 subgroups for each characteristic variable.

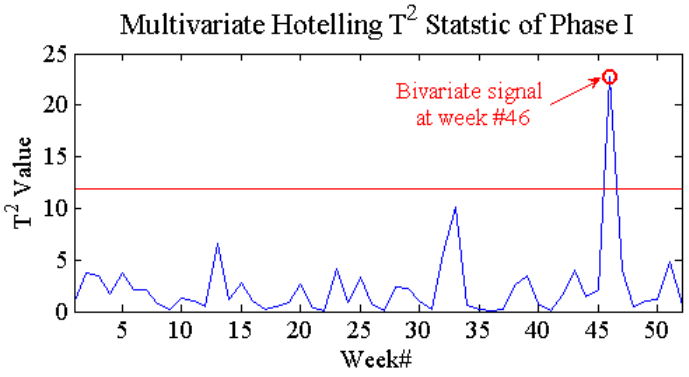


FIGURE 4 $T^2$ Control Chart of Displ-L & Displ-T in Phase *I*

We constructed a $T^2$ control chart in Phase *I* by laying the first 52 samples of $T^2$ statics over a horizontal line in Figure 4. The superimposed upper control limit (UCL) was calculated by equation (14), where the type-I error rate was set as $\alpha = 0.27\%$ to keep consistence with the $3\sigma$ boundaries widely used in quality monitoring.

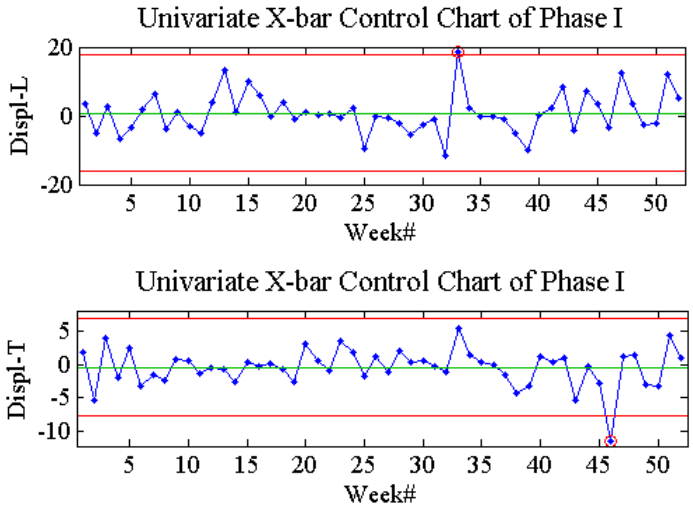


FIGURE 5 Univariate Control Chart of Displ-L & Displ-T in Phase *I*

Figure 4 shows that an out-of-control point is signaled at sampling week #46. In order to make comparisons, we also plotted the univariate control charts separately for Displ-L and Displ-T in Figure 5. The control limits in the univariate charts were set as $3\sigma$ away from the center line (i.e., $\alpha = 0.27\%$). The results indicate an out-of-control signal at sampling week #33 in Displ-L as well as another out-of-control signal at sampling week #46 in Displ-T. It means that the signal in the $T^2$ control chart is explained by the unusual change in Displ-T, while it barely passes the unusual change is Displ-L. A plausible explanation argues that the signal in Displ-T in week #46 is farther beyond the control limit than the one in Displ-L in week #33. To better understand this different treatment, we constructed a 2-D data plane as shown in Figure 6.

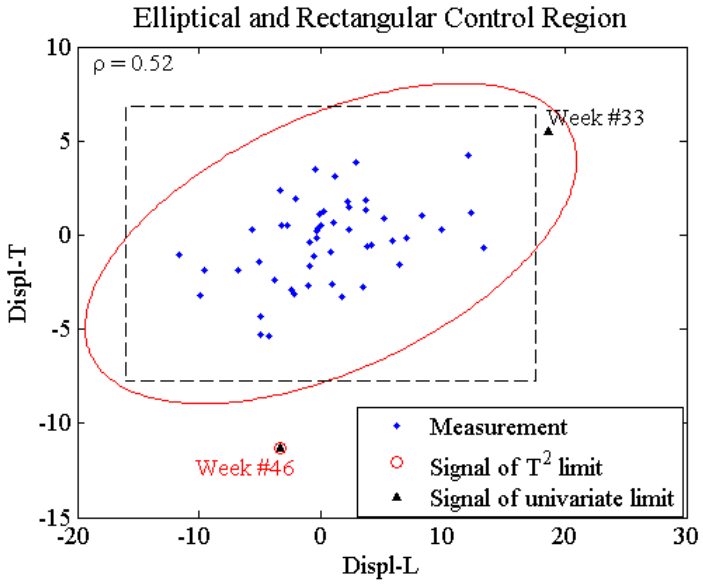


FIGURE 6 Elliptical and Rectangular Control Region of Displ-L & Displ-T in Phase *I*

The horizontal axis in Figure 6 corresponds to the innovation values of Displ-L, and the vertical axis corresponds to the innovation values of Displ-T. Therefore, any point on the 2-D data plan represents a bivariate sample in the Phase *I* data set. In addition, we drew the two sets of control limits which shape a rectangular region (dashed line). Not surprisingly, a point outside this rectangle represents an out-of-

control signal detected by the univariate control charts. For example, in week #33, the point falls to the right of the rectangle, indicating that it falls beyond the UCL of Displ-L. On the other hand, the $T^2$ control limit corresponds to a tilted ellipse in the data plane (solid line) as is suggested in section 2.3. It is worth noting that when the bivariate samples are independent to each other, the ellipse will be flat. And it becomes increasingly tilted when the samples are increasingly correlated. Similarly, any point outside the ellipse represents an out-of-control signal in the $T^2$ control chart.

The graphic layout in Figure 6 helps to explain why week #33 is not signaled in the $T^2$ control chart. In fact, this happens because: in order to achieve an equivalent overall type-I error rate, the univariate charts are slightly more conservative than the $T^2$ chart on both axes. In other word, the $T^2$ chart pays addition attention to the deviation from the established correlation structure, and as a trade-off, it is slightly more liberal to univariate outliers.

### 3.2 Interpretation of Signals

Now suppose neither the univariate control charts nor the 2-D data plane are conveniently available (which is true when the number of distresses is larger than two), we used the MYT decomposition technique to interpret the signal in Figure 4 from a statistical perspective. Following the method described in section 2.4.1, we decomposed the $T^2$ value in sampling week #46 in Table 2. Here we denote the marginal (i.e. unconditional) contribution of Displ-L to the $T^2$ value as $T_1^2$ and the marginal contribution of Displ-T as $T_2^2$. Meanwhile, we denote the conditional contribution of Displ-T as $T_{2|1}^2$ when Displ-L is fixed and vice versa. Remember that the components follow the relationship:

$$T^2 = T_1^2 + T_{2|1}^2 = T_2^2 + T_{1|2}^2$$

TABLE 2 MYT Decomposition of $T^2$ Statistic for Displ-L & Displ-T

| Signal | $T^2$ | Unconditional | | Conditional | |
|---|---|---|---|---|---|
| | | $T_1^2$ | $T_2^2$ | $T_{2\|1}^2$ | $T_{1\|2}^2$ |
| #46 | 22.77 | 0.5 | 19.29 | 22.27 | 3.48 |
| | | *Critical value: 8.97 ($\alpha = 0.27\%$)* | | | |

Moreover, we set the confidence level as $\alpha = 0.27\%$ and obtained the critical value for both the marginal and conditional $T^2$ components and provided it at the bottom of Table 2. We can see that both the marginal and conditional components of Displ-T (i.e., $T_2^2$ and $T_{2|1}^2$) significantly exceeds the critical value. In contrast, both components regarding Displ-L stay comfortably below the critical value. As a result, it is reasonable to state that Displ-T has significantly contributed to the large value of $T^2$ at sampling week #46, and should be further investigated for plausible causes.

Finally, we removed the sample in week #46, re-estimated the control limit and constructed the $T^2$ control chart again. It turns out that the rest of Phase *I* data are within the updated control limit, which in a bivariate sense indicates an in-control process where no unusual change occurs.

Therefore, it is reliable to use this historic data set to estimate the control limits for Phase *II* monitoring. We calculated the UCL for Phase *II* by equation (16) and an overall $T^2$ control chart including both phases is illustrated in Figure 7. Since none of the samples is beyond the control limit, we conclude that the bivariate displacement behaviors show no unusual changes over the 89 weeks except for

the previously removed sample in week #46. This single outlier physically means that Girder 1 unusually moved southbound over the week of Feb. 7th in 2011.

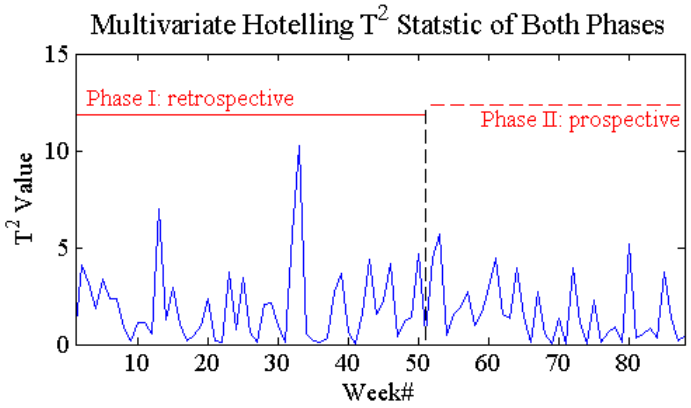


FIGURE 7 $T^2$ Control Chart of Displ-L & Displ-T in Both Phase *I* and Phase *II*

## 4. CONCLUSIONS

The statistical framework we proposed uses multivariate statistical process control techniques to monitor multiple facility distresses simultaneously. Specifically, it employs Hotelling's $T^2$ control chart to synthesize multivariate measurement series to a scalar series that is convenient to compute, compare, visualize and manage. In addition, we described the MYT decomposition technique to find plausible causes for the out-of-control signals in the $T^2$ control chart. We implemented the framework to monitor multiple distresses on the Hurley Bridge and illustrated the results on a biaxial displacement pair to validate the detecting capability of the framework.

## 5. REFERENCES

[1] Chen, Y., Corr, D. and Durango-Cohen P. Analysis of Common-cause and Special-cause Variation in the Deterioration of Transportation Infrastructure: A Field Application of Statistical Process Control for Structural Health Monitoring. Submitted to Transportation Research Part B: Methodological.

[2] Hotelling, H. Multivariate Quality Control – Illustrated by the Air Testing of Sample Bombsights. *Techniques of Statistical Analysis*, C. Eisenhart, M. Hatay, and W.Wallis, eds., McGraw Hill, New York, NY, pp. 111-184.

[3] Mahalanobis, P. On Tests and Measures of Group Divergence. *Journal of the Asiatic Society of Bengal*, Vol. 26, 1930, pp. 541-588.

[4] Alwan, L.C. *Statistical Process Analysis*, McGraw-Hill, 2000.

[5] Alt, F. B., Smith, N. D., and Jain, K. Multivariate Quality control. *Handbook of Statistical Methods for Engineers and Scientists*, Second Edition, J. Wadsworth, Harrison M., eds., McGraw-Hill, New York, NY, 1990.

[6] Shewhart, W. *Economic Control of Quality of Manufactured Products*. Van Nostrand Company, New York, NY, 1931.

[7] Alt, F. B. Multivariate Quality Control: State of the Art. *ASQC Annual Quality Congress Transactions*, 1982, pp. 886-893.

[8] Lowry, C. A. and Montgomery, D. C. A Review of Multivariate Control Charts. *IIE Transactions*, Vol. 27, No. 6, 1995, pp. 800-810.

[9] Bersimis, S., Panaretos, J., and Psarakis, S. Multivariate Statistical Process Control Charts and the Problem of Interpretation: A Short Overview and Some Applications in Industry. *Proceedings of the 7th Hellenic European Conference on Computer Mathematics and its Applications*, Athens, Greece, 2005.

[10] Bersimis, S., Psarakis, S., and Panaretos, J. Multivariate Statistical Process Control Charts: An Overview. *Quality & Reliability Engineering International*, Vol. 23, No. 5, 2006, pp. 517-543.

[11] Mason, R. L., Tracy, N. D., and Young, J. C. Decomposition of $T^2$ for Multivariate Control Chart Interpretation. *Journal of Quality Technology*, Vol. 27, No. 2, 1995, pp. 109-119.

[12] Mason, R. L., Champ, C. W., Tracy, N. D., Wierda, S. J., and Young, J. C. Assessment of multivariate process control techniques. *Journal of Quality Technology*, Vol. 29, No. 2, 1997, pp. 140-143.